

# Can mass change the diffusion coefficient of DNA-coated colloids?

Sophie Marbach<sup>1,2</sup> and Miranda Holmes-Cerfon<sup>1</sup>

<sup>1</sup>*Courant Institute of Mathematical Sciences, New York University, NY, 10012, U.S.A.*

<sup>2</sup>*CNRS, Sorbonne Université, Physicochimie des Electrolytes et Nanosystèmes Interfaciaux, F-75005 Paris, France \**

Inertia does not generally affect the long time diffusion of passive overdamped particles in fluids. Yet we have discovered a surprising property of particles coated with ligands, that bind reversibly to surface receptors – heavy particles diffuse more slowly than light ones of the same size. We show this by simulation and by deriving an analytic formula for the mass-dependent diffusion coefficient in the overdamped limit. We estimate the magnitude of this effect for a range of biophysical ligand-receptor systems, and find it is potentially observable for microscale DNA-coated colloids.

It is well known that inertia does not affect either the equilibrium probabilities or dynamics in overdamped systems [1], and especially that it does not affect the long time diffusion of micron-scale particles in liquids at equilibrium [2]. In fact, momentum relaxation for microscale particles occurs over a timescale of order  $1 \mu\text{s}$  [3]. Particles are generally observed on much longer timescales, where the motion at equilibrium appears overdamped and diffusive, with diffusion coefficient independent of mass for large enough particles [4, 5]. Inertia can only affect the short-time mobility of a particle [2, 5], and it can play a role for active particles where  $\tau_m$  is comparable to the diffusive rotational timescale, which is only accessible experimentally for active particles in air (not in liquids) [6]. Therefore, to our knowledge, there is currently no proposed physical system where inertia could affect long time diffusion of microscale particles in liquids at equilibrium.

Yet, as soon as another timescale, originating from an additional complexity of the system, is of the same order as the inertial relaxation timescale, one might ask whether the mobility of the system could depend on its mass [2, 4–12]. One widespread example of an overdamped system with an additional fast timescale is particles with ligand-receptor contacts, such as colloids functionalized with DeoxyriboNucleic Acid (DNA) stickers [13–15], viruses [16–19] or white blood cells [20–22]. Such particles are coated with sticky ligands that bind and unbind to receptors on an opposing surface (Fig. 1), which changes the relative mobility between the particle and the surface [14, 16, 23, 24]. The ligand binding and unbinding rates can be fast, so one might speculate that when they occur on the same timescale as the relaxation of the ambient fluid’s momentum, the coupling between these two effects, which both act on the particle’s momentum, could induce inertial effects. For example, bimolecular reactants with inertia can show different survival probability decay functions depending on their mass [25, 26]. Furthermore, we have recently pointed out that models of DNA-coated colloids find different long-time diffusion coefficients when they start with the underdamped Langevin equation for particle motion, as

in Ref. [27], or from the overdamped equation, as in Ref. [28]. For stiff ligands, where motion is strongly suppressed when the ligand is bound to a surface receptor, the particle’s diffusion coefficient is significantly reduced when it is underdamped compared to when it is overdamped (Fig. 1). We therefore ask: could inertia affect the long-time diffusion of particles with ligand-receptor contacts? Can we quantify the magnitude of the effect and predict its onset for existing biophysical systems?

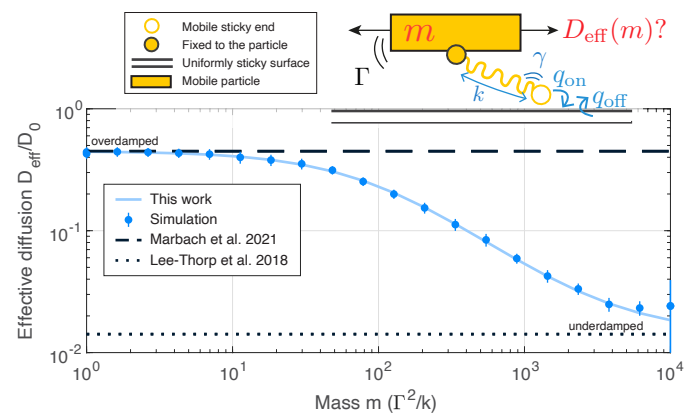


**FIG. 1. Mass changes the diffusion coefficient of a particle with 1-ligand.** Numerically obtained long time diffusion coefficient  $D_{\text{eff}}$  of a plate of mass  $m$  with bare friction coefficient  $\Gamma$ , with a single ligand - called here leg. The leg has friction coefficient  $\gamma$  and spring constant  $k$ . It binds and unbinds with rates  $q_{\text{on}}$  and  $q_{\text{off}}$  to a uniformly sticky surface. Limit behaviors derived in previous works from the overdamped Langevin equation for the particle in Ref. [28] (dashed) and from the underdamped Langevin equation in Ref. [27] (dotted). “This work” refers to Eq. (5). Error bars correspond to one standard deviation for 20 independent simulations. Parameters for the simulations are  $q_{\text{on}} = 0.01k/\Gamma$ ,  $q_{\text{off}} = 0.008k/\Gamma$ ,  $\gamma = \Gamma$ .

We address these questions by investigating a minimal model that includes the essential ingredients of (a) inertial relaxation and (b) stochastic dynamics of binding and unbinding. We consider an  $N$ -legged particle of mass  $m$ , with spring-like legs representing the ligands [29–31], and a sticker at the tip of each leg that may transiently attach to a uniformly sticky surface – see Fig. 1. Legs attach independently to the surface with rate  $q_{\text{on}}$  and

\* sophie@marbach.fr

detach with rate  $q_{\text{off}}$ , where both rates are here taken constant for simplicity. Inertia of the legs may be neglected as in general legs are much lighter than the particle (see also Supplementary 2.4 for a detailed justification). The particle's motion is investigated in 1D, on the lateral dimension parallel to the surface axis. The dynamical equations for the unbound leg lengths  $l_j$  are

$$\frac{dl_j}{dt} = -\frac{k}{\gamma}(l_j - l_0) + \sqrt{\frac{2k_B T}{\gamma}}\eta_j, \quad (1)$$

where  $k$  is a spring constant,  $l_0$  is a rest length and  $\gamma$  is the friction coefficient of each leg. The  $\eta_j$  are uncorrelated white gaussian noises, such that  $\langle \eta_j(t)\eta_k(t') \rangle = \delta_{kj}\delta(t-t')$  and  $\langle \eta_j(t) \rangle = 0$  where  $\langle \cdot \rangle$  is an average over realizations of the noise. The bound legs  $l_i$  are constrained to move at the same speed as the particle,  $v = dx/dt$ , where  $x$  is the particle position:

$$\frac{dx}{dt} = \frac{dl_i}{dt} = v. \quad (2)$$

Finally, the particle's velocity is governed by Newton's law, including friction and stochastic forces on the particle induced by the ambient fluid, as well as friction, recall and stochastic forces originating from the bound legs

$$m\frac{dv}{dt} = -\Gamma v + \sqrt{2k_B T\Gamma}\eta_x + \sum_{i \in \text{bound}} \left( -\gamma v - k(l_i - l_0) + \sqrt{2k_B T\gamma}\eta_i \right). \quad (3)$$

Here the  $\eta_i$  and  $\eta_x$  are further uncorrelated white gaussian noises and  $i$  is a running index over currently bound legs. Note that for a particle in fluid the relevant mass scale in Eq. (3) is  $m \rightarrow m + m_f/2$  where  $m_f$  is the mass of the displaced volume of fluid [2, 32]. We remark that compared to a starting point with overdamped equations for both the leg and the particle, here it is not necessary to project the unbound dynamics to obtain the bound dynamics [28, 33]; Newton's law is sufficient.

The Langevin dynamics in Eq. (3) are our starting point to investigate the effect of inertia [11, 34]. We recall that in fluids of similar density as the particle – as is mostly envisioned here, except for *e.g.* gold colloids in water or viruses in air – momentum relaxes algebraically instead of exponentially and thus the effective decay of inertial effects is even slower than predicted with Langevin dynamics [2]. Capturing this algebraic decay generally requires solving for the full flow field of the solvent and is therefore not suitable for analytic investigation, however, we expect our model will give a lower bound on the effect of inertia, and is therefore suited to explore the onset of inertial effects.

Stochastic simulations of our model show that the long time diffusion strongly depends on mass. As an example, we show in Fig. 1, the long time diffusion coefficient calculated as

$$D_{\text{eff}} \underset{t \gg \tau_{\text{max}}}{=} \frac{\langle x^2(t) \rangle}{2t} \quad (4)$$

of a particle with  $N = 1$  leg, where  $\tau_{\text{max}}$  is the longest physical timescale in the model (see Supplementary 1).  $D_{\text{eff}}$  continuously decreases with particle mass, between the two limit regimes identified respectively in Ref. [28] (overdamped) and Ref. [27] (underdamped), by more than an order of magnitude.

To further understand how this decrease depends on the model parameters ( $N, k, q_{\text{on}}, q_{\text{off}}, \gamma, \Gamma$ ), we derive an analytic expression for  $D_{\text{eff}}$  by considering the overdamped limit of the combined particle and leg dynamics. We begin by introducing the 5 nondimensional scales

$$x \rightarrow L_x \tilde{x}, \quad l_i - l_0 \rightarrow \tilde{L}_i, \quad t \rightarrow \tau \tilde{t}, \quad v \rightarrow V \tilde{v}, \quad m \rightarrow M \tilde{m}.$$

Here  $L = \sqrt{k_B T/k}$  is the characteristic length of leg fluctuations, while  $L_x$  and  $\tau$  are respectively the lengthscale and timescale for the long-time motion of  $x$ . In contrast with other works [35, 36], the latter two scales are not determined *a priori* by any intrinsic scales. Rather, they are chosen large enough that coarse-graining will be appropriate over such scales and will lead to diffusive dynamics [28]. Hence we choose  $L_x = L/\epsilon$  where  $\epsilon \ll 1$  is a small nondimensional number, and  $\tau = L_x^2/D_0$ , which corresponds to  $\tau = \frac{1}{\epsilon^2} \frac{\Gamma}{k}$ . Velocity fluctuations are fast compared to diffusive motion such that  $V = L_x/\tau\epsilon$ .

Importantly, we must specify the scale of mass by comparing the velocity auto-correlation time  $\tau_v$  to  $\tau$ . One choice is to relate  $\tau_v$  to the recall spring force, as  $\tau_v = MV/(Lk)$  [27]. If we require  $\tau_v$  to be much smaller than the observation timescale, say  $\tau_v = \epsilon^2\tau$  then we obtain  $\tau_m = M/\Gamma = \Gamma/k\epsilon^2$ . This implies the inertial relaxation  $\tau_m$  is very large compared to the relaxation of leg fluctuations, typical of an *underdamped* motion, and is therefore not the appropriate scale to consider. Instead we consider another choice, *i.e.* the velocity auto-correlation time in the absence of recall forces  $\tau_v = \tau_m = M/\Gamma$  and consider that it is small compared to the observation time  $\tau_v = \tau_m = \epsilon^2\tau$ . Note that the latter scaling is the usual scaling to obtain *overdamped*, or more generally long time diffusive, dynamics [37].

Finally, we observe the system at sufficiently long times such that the remaining timescales are much shorter:  $\gamma/k \sim \Gamma/k \sim q_{\text{on}}^{-1} \sim q_{\text{off}}^{-1}$ . We thus can take  $q_{\text{on}} \rightarrow \frac{\tau}{\tilde{\epsilon}^2} \tilde{q}_{\text{on}}$  and similarly for  $q_{\text{off}}$ .

We use our hierarchy of scales to coarse-grain the dynamics of the system specified through Eqns. (1-3). The equations have an associated backward Kolmogorov equation  $\partial_t f = \mathcal{L}f$ , where  $f$  is a vector-valued function with  $2^N$  components corresponding to all the possible bond states and  $\mathcal{L}$  is the generator of the system. Inferring the long-time dynamics of  $f$  is sufficient to infer the long-time dynamics of the particle. The non-dimensional backward equation is (dropping the  $\tilde{\cdot}$  for simplicity)  $\partial_t f = \mathcal{L}f = \frac{1}{\epsilon^2}\mathcal{L}_0 f + \frac{1}{\epsilon}\mathcal{L}_1 f$ . We seek a solution to this equation in the form of an expansion in  $\epsilon$ ,  $f = f_0 + \epsilon f_1 + \epsilon^2 f_2 + \dots$ . Standard coarse-graining steps (Supplementary 2) allow us to establish long time overdamped dynamics on  $f_0$  [27, 28, 35, 37]. We find that the system diffuses with a diffusion coefficient, independent

of  $\epsilon$ , as

$$D_{\text{eff}}(m) = \frac{k_B T}{\Gamma_{\text{eff}}(m)} = \sum_{n=0}^N p_n \frac{k_B T}{\Gamma_n(m)} \quad (5)$$

where  $p_n = \binom{N}{n} \frac{q_{\text{on}}^n q_{\text{off}}^{N-n}}{(q_{\text{on}} + q_{\text{off}})^N}$  is the probability to have  $n$  bonds and  $\Gamma_n(m)$  are the effective friction coefficients contributing to a state with  $n$  bonds. The  $\{\Gamma_n\}$  satisfy a linear system of equations involving the mass of the particle  $m$  that is reported in Supplementary 2. Importantly, Eq. (5) predicts up to order of magnitude changes on the effective diffusion  $D_{\text{eff}}$  depending on the specific microscopic parameter values.

Let us analyze in detail a  $N = 1$ -legged particle. The system determining  $\{\Gamma_n\}$  can be solved analytically to obtain friction coefficients for the bound and unbound states

$$\begin{aligned} \frac{\Gamma_0(m)}{\Gamma} &= 1 + \frac{mq_{\text{on}}}{\Gamma} \frac{\gamma_{\text{eff}}}{\gamma_{\text{eff}} + \Gamma + m(q_{\text{on}} + q_{\text{off}})}, \\ \frac{\Gamma_1(m)}{\Gamma} &= 1 + \frac{\gamma_{\text{eff}}}{\Gamma} \frac{\Gamma + mq_{\text{on}}}{\Gamma + m(q_{\text{on}} + q_{\text{off}})}. \end{aligned} \quad (6)$$

Here  $\gamma_{\text{eff}} = \gamma + k \left( \frac{1}{q_{\text{off}}} + \frac{\gamma}{k} \frac{q_{\text{on}}}{q_{\text{off}}} \right)$  is the effective friction from the leg, including the leg's bare friction  $\gamma$  and recall forces from the tethered spring. The coefficients satisfy  $\Gamma_0 \leq \Gamma_1$  as, when it is bound, the leg exerts additional recall forces on the particle. We compare our analytic result for  $D_{\text{eff}} = k_B T / \Gamma_{\text{eff}}$  with direct stochastic simulations over a wide range of parameters and find excellent agreement (Figs. 1 and 2A). Overall, the effective friction  $\Gamma_{\text{eff}}$  increases with mass, and therefore the particle's diffusive motion slows down with increased mass.

Eq. (6) gives insight into what controls both the onset of the diffusion slow down, and the magnitude of the effect. Diffusion begins to decrease when the binding and unbinding times  $\tau_{\text{on}} = q_{\text{on}}^{-1}$ ,  $\tau_{\text{off}} = q_{\text{off}}^{-1}$  become small enough to be comparable with the relaxation time of inertia,  $\tau_m = m/\Gamma$ . This is also apparent in Fig. 2A where the transition between limit regimes systematically occurs for  $mq_{\text{on}}/\Gamma \sim 1$ . For shorter binding times,  $\tau_{\text{on}} \sim \tau_{\text{off}} \ll \tau_m$ , inertial effects matter, and the friction coefficients converge to (using the notation  $m = \infty$  for  $m \gg \Gamma/q_{\text{on}}, \Gamma/q_{\text{off}}$ )

$$\frac{\Gamma_0^{m=\infty}}{\Gamma} = \frac{\Gamma_1^{m=\infty}}{\Gamma} = 1 + p_1 \frac{\gamma_{\text{eff}}}{\Gamma}. \quad (7)$$

The friction coefficients contributing to each state are the same, regardless of the state (bound or unbound) of the particle. This is coherent: since the particle has significant inertia, it does not have the time to accelerate or decelerate to a different dynamical regime upon changing state. Binding and unbinding happen too rapidly for the particle to sense differences. Eq. (7) was also obtained in Ref. [27] which started with the underdamped equations and the scaling  $\tau_v = MV/(Lk)$ .

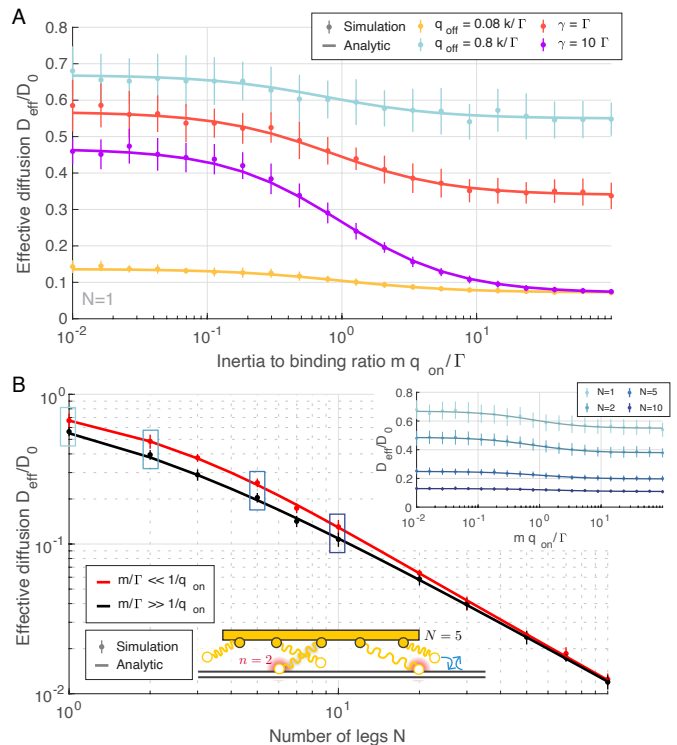


**FIG. 2. Diffusion slow down controlled by the ratio of inertial to binding timescales,  $mq_{\text{on}}/\Gamma$ .** (A) Effective diffusion for a  $N=1$ -legged particle with respect to the inertia to binding ratio, from direct stochastic simulations and analytic Eq. (5), with friction coefficients given by Eq. (6). (B) Effective diffusion with respect to the number of legs  $N$ , in the large or small mass limit, from direct stochastic simulations and analytic Eq. (5) (solving numerically the linear system for the  $\{\Gamma_n\}$ ) with  $mq_{\text{on}}/\Gamma = 0.01$  (red) and  $mq_{\text{on}}/\Gamma = 100$  (black). (top inset) Effective diffusion relative to inertia to binding ratio, for different  $N$ . (bottom inset) Schematic of a mobile particle with  $N$  legs including  $n$  bound legs to the surface. Other simulation parameters are  $\gamma = 0.1\Gamma$ ,  $q_{\text{off}} = 0.8k/\Gamma$ , and  $q_{\text{on}} = k/\Gamma$ . Error bars correspond to one standard deviation for 100 independent simulations.

Reciprocally, if binding timescales are long compared to inertial relaxation ( $\tau_{\text{on}} \sim \tau_{\text{off}} \gg \tau_m$ ) we expect inertia to play a negligible role: the particle has the time to accelerate and reach an overdamped, limit motion before any further change of state occurs. In this case the friction coefficients are

$$\frac{\Gamma_0^{m=0}}{\Gamma} = 1, \quad \frac{\Gamma_1^{m=0}}{\Gamma} = 1 + \frac{\gamma_{\text{eff}}}{\Gamma}. \quad (8)$$

Eq. (8) was obtained in Ref. [28], starting directly with overdamped motion of the particle.

We therefore find that the onset of inertial effects is governed by the ratio of timescales,  $\tau_{\text{on}} \sim \tau_{\text{off}}$  compared to  $\tau_m$ . *A posteriori*, it is natural that this onset is controlled by timescales, yet it was not obvious *which* of the diversity of timescales at play in ligand-receptor systems would matter. For example, the timescale for relaxation

of leg fluctuations  $k/\gamma$  does not control the occurrence of inertial slow-down.

However,  $k/\gamma$  does control the magnitude of the inertial slow-down, via  $\gamma_{\text{eff}}$ . The relative slow down between the underdamped and the overdamped regime is indeed

$$\frac{D_{\text{eff}}^{m=\infty}}{D_{\text{eff}}^{m=0}} = \frac{1 + \frac{\gamma_{\text{eff}}}{\Gamma}}{1 + \frac{\gamma_{\text{eff}}}{\Gamma} + p_0 p_1 \frac{\gamma_{\text{eff}}^2}{\Gamma^2}}. \quad (9)$$

If the leg is very stiff ( $k \gg \Gamma q_{\text{off}}$ , implying  $\gamma_{\text{eff}} \gg \Gamma$ ), then diffusion can be significantly slowed for massive particles,  $D_{\text{eff}}^{m=\infty} \ll D_{\text{eff}}^{m=0}$ . In fact, stiff legs greatly reduce motion in the bound state,  $\Gamma_1 \gg \Gamma$ . Since a particle with large mass does not have the time to accelerate while its leg is unbound, we also have increased friction in the unbound state  $\Gamma_0^{m=\infty} \gg \Gamma$  and the particle's overall mobility is decreased, by up to orders of magnitude (as seen in Fig. 1). For an overdamped particle, on the contrary, even with a stiff leg, the particle can still move when it is unbound, as it has time to accelerate ( $\Gamma_0^{m=0} = \Gamma$ ), and its diffusion coefficient remains finite.

Let us now consider a particle with many legs involved in the binding process, say  $N \approx 100 - 1000$ , as in some DNA-coated colloids at low temperatures [38, 39]. The linear system satisfied by  $\{\Gamma_n\}$  can be simplified when the average number of bonds is large,  $\bar{N} = \frac{q_{\text{on}}}{q_{\text{on}} + q_{\text{off}}} N \gg 1$ , to

$$\Gamma_{\text{eff}}(m) \underset{\bar{N} \gg 1}{\simeq} \Gamma + \bar{N} \gamma_{\text{eff}}. \quad (10)$$

Now the diffusion coefficient does not depend on the mass of the particle. Stochastic simulations, as well as numerical solutions of the linear system satisfied by the  $\{\Gamma_n\}$ , confirm this result: the diffusion coefficient at large number of legs  $N$  converges to a value independent of mass (Fig. 2B). Interestingly, the transition to the slowed-down diffusion regime occurs when  $\tau_m/\tau_{\text{on}} \propto N$  (Supplementary 2.3.3).

Why do inertial effects vanish with a large number of legs? For a particle with large mass, the friction coefficients for each state are equal (as in Eq. (7) for the 1-legged case), because the particle does not have time to accelerate between changes, and hence is only sensitive to the average configuration:  $\Gamma_0^{m=\infty} = \Gamma_1^{m=\infty} = \dots = \Gamma_{\bar{N}}^{m=\infty} = \Gamma + \bar{N} \gamma_{\text{eff}}$  (Supplementary 2.3.2). The difference is that now an average of  $\bar{N}$  legs exerts extra recall forces. For a particle with very small mass, friction coefficients for each state are different, but their sum in Eq. (5) is dominated by the most likely state, which is  $\bar{N}$  when this average is large, leading to  $\Gamma_{\text{eff}}^{m=0} \approx \Gamma_{\bar{N}}^{m=0} = \Gamma + \bar{N} \gamma_{\text{eff}}$ . Numerous legs can thus be thought of as self-averaging, and hence transitions between states do not matter as much as when there are a small number of bound legs.

We now explore the possible emergence of such inertial effects in biological or biomimetic systems. Within our theory, the inertial relaxation time  $\tau_m = m/\Gamma$  is quite fast: for a  $R \sim 1 \mu\text{m}$  particle near a surface,  $\Gamma \sim 2 \times 6\pi\eta R \sim 10^{-8} \text{ kg/s}$  with water viscosity  $\eta \sim 10^{-3} \text{ Pa}\cdot\text{s}$

and  $m \sim \rho \frac{4}{3} \pi R^3 \sim 10^{-15} \text{ kg}$  with density  $\rho \sim 10^3 \text{ kg/m}^3$ , such that  $\tau_m = m/\Gamma \sim 100 \text{ ns}$ , accumulating to slightly longer timescales if we account for the momentum relaxation of the fluid [2]. In any case, to observe inertial effects, the typical binding times ( $\tau_{\text{on}} = q_{\text{on}}^{-1}$ ,  $\tau_{\text{off}} = q_{\text{off}}^{-1}$ ) have to be faster. As typical adhesive systems have at least  $q_{\text{off}} \lesssim 10 q_{\text{on}}$ , we focus mainly on  $q_{\text{on}}$  in the following, as it will be the limiting binding rate affecting  $D_{\text{eff}}$ . We report the orders of magnitude for the momentum relaxation time  $\tau_m = m/\Gamma$  and binding times  $\tau_{\text{on}} = q_{\text{on}}^{-1}$  for a variety of multivalent ligand-receptor systems – see Fig. 3 (and details in Supplementary 3.2). To keep the discussion simple we limit ourselves to a small number of average bound legs  $\bar{N} \simeq 1$ , which is inherent or can be achieved (*e.g.* with temperature control [39]) in all systems explored.

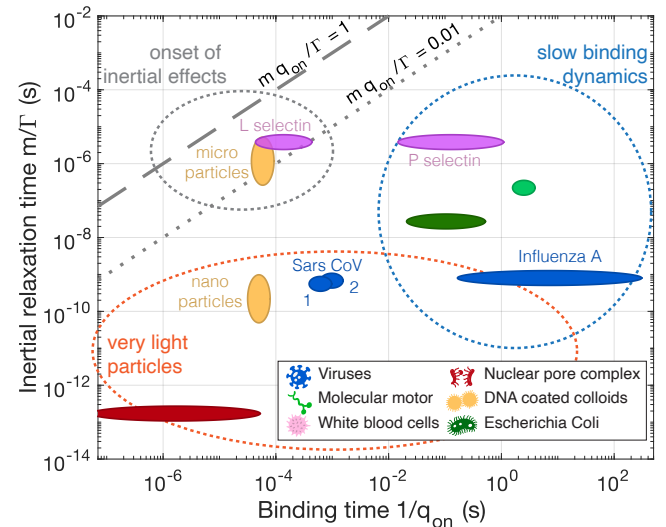


FIG. 3. **Sorting biophysical systems.** Ashby chart comparing the typical inertia versus binding timescales for various systems. Full disks represent the range of values found in the literature for each system. Systems are color coded according to their category in the legend. When multiple systems belong to a category, details are indicated next to the circles. Large dashed circles represent global categories of systems.

Numerous multivalent ligand-receptor systems – such as spike proteins on the Influenza A virus [40, 41], molecular motors transporting cargos [42] or pili adhesion of Escherichia Coli [43–45] – have binding kinetics that are simply too slow to observe inertial effects, typically  $q_{\text{on}} \lesssim 100 \text{ s}^{-1}$ . Such slow binding prevents inertial slow down (blue dashed circle in Fig. 3). These systems are indeed overdamped.

Other systems do have fast binding kinetics ( $q_{\text{on}} \gtrsim 10^4 \text{ s}^{-1}$ ), but not fast enough to incur inertial effects on the lighter systems they are connected to. These often correspond to smaller particles, and since  $m/\Gamma \propto R^2$ , this decreases the maximum binding timescale required to observe inertial effects. This is the case of Sars CoV 1 and 2 viruses that are barely  $R = 50 \text{ nm}$  in radius [46, 47],

of DNA-coated nanocolloids that have particle radii in the  $R = 10$  nm range [48] and of protein transporters in the nuclear pore complex [49] (orange dashed circle in Fig. 3). Some systems are both light and with slow binding kinetics, as is the case of *e.g.* Influenza A, and hence are also overdamped.

Inertial effects may therefore occur for a specific combination of large particles and fast binding kinetics. We have isolated two systems for which such a combination may be obtained: (a) DNA-coated colloids near the melting point, where the colloids are micron-sized ( $R \sim 1\mu\text{m}$ ) and (b) white blood cells with adhesion mediated by the L-selectin protein only – see Table. S1. For both these systems, typical existing experimental designs possess an inertial time to binding time ratio  $m q_{\text{on}}/\Gamma \simeq 10^{-3} - 10^{-1}$ , which is already within, or close to, the range where we predict inertial slow down – see Fig. 2.

DNA-coated colloids offer a promising route to probe such inertial slow down as they may be finely tuned to increase the inertial relaxation time, for example by using coating processes on gold particles [38] (to increase  $m$ ), larger particles [39] (to increase the ratio  $m/\Gamma \propto R^2$ ) or by modifying the viscosity of the solution (to alter  $\Gamma$ ). The average number of bound legs  $\bar{N}$  for DNA-coated colloids can also be tuned over a wide range ( $\bar{N} = 1 - 1000$ ), for example by using different coating densities on either surface, or by changing temperature [39]. With typical experimental parameters [28, 39, 50], Eq. (9) predicts a slow down of  $D_{\text{eff}}^{m=\infty}/D_{\text{eff}}^{m=0} \simeq 92\%$ , which could be amenable to experimental measurements (see Supplementary 3.1). Note that targeted experimental designs (such as stiffer legs) could produce a greater decrease. Therefore, we expect that inertial slow down of the long-time diffusion coefficient could be probed with existing experimental techniques on DNA-coated colloids.

In summary, we have found that inertia can modify the diffusion coefficient of particles with ligand-receptor contacts, inducing a diffusion slow-down with increased inertia. Within our analytic framework, the onset of this slow-down occurs when the binding time scale  $\tau_{\text{on}} = q_{\text{on}}^{-1}$  is faster than the timescale for the inertial relaxation, which is  $\tau_m = m/\Gamma$  in our model, a lower bound on the

actual timescale since momentum decays algebraically in most fluid systems [2, 5]. The magnitude of the effect is controlled by the stiffness of the ligands and the average number of bound legs, with stiff ligands and fewer bound legs promoting increased inertial effects. We predict the diffusion slow down could be probed experimentally by fine-tuning existing DNA-coated colloids. Such experiments may also give further insight into the coupled dynamics between the solvent and the ligand-receptor binding dynamics, and identify other inertial effects, beyond diffusion slow down. For example, in dense active suspensions, particles need time to pick up speed after collisions, which modifies both their long time diffusion [6] and phase separation behavior [12]. Improvements to our model could include fluid memory kernels to investigate the decay of velocity autocorrelation functions [2] or inhomogeneities in the lateral direction to probe inertial effects on the subdiffusion regime [38]. For DNA-coated colloids, one could envision that such inertia-modified dynamics could also impact collective properties such as crystallographic alignment into self-assembled structures [33, 51]. Understanding the dynamics of such complex microscale particles is a key step to pave the way towards controlled design at the microscale, *e.g.* to improve synthesis of materials with advanced optical properties [52, 53].

## ACKNOWLEDGMENTS

The authors acknowledge fruitful discussions with Aleksandar Donev and Brennan Sprinkle. S.M. acknowledges funding from the MolecularControl project, European Union’s Horizon 2020 research and innovation programme under the Marie Skłodowska-Curie grant award number 839225. All authors were supported in part by the MRSEC Program of the National Science Foundation under Award Number DMR-1420073. M.H.-C. was partially supported by the US Department of Energy under Award No. DE-SC0012296, and acknowledges support from the Alfred P. Sloan Foundation.

- 
- [1] M. E. Cates and V. N. Manoharan, Celebrating Soft Matter’s 10th anniversary: Testing the foundations of classical entropy: colloid experiments, *Soft Matter* **11**, 6538 (2015).
  - [2] X. Bian, C. Kim, and G. E. Karniadakis, 111 years of brownian motion, *Soft Matter* **12**, 6331 (2016).
  - [3] See order of magnitude derivation in Supplementary 3.1.
  - [4] J. Schmidt and J. Skinner, Hydrodynamic boundary conditions, the stokes-einstein law, and long-time tails in the brownian limit, *The Journal of chemical physics* **119**, 8062 (2003).
  - [5] F. Balboa Usabiaga, X. Xie, R. Delgado-Buscalioni, and A. Donev, The stokes-einstein relation at moderate schmidt number, *The Journal of chemical physics* **139**, 214113 (2013).
  - [6] H. Löwen, Inertial effects of self-propelled particles: From active brownian to active langevin motion, *The Journal of chemical physics* **152**, 040901 (2020).
  - [7] T. Li and M. G. Raizen, Brownian motion at short time scales, *Annalen der Physik* **525**, 281 (2013).
  - [8] A. Daddi-Moussa-Ider, A. Guckenberg, and S. Gekle, Long-lived anomalous thermal diffusion induced by elastic cell membranes on nearby particles, *Physical Review E* **93**, 012612 (2016).
  - [9] M. Trulsson, B. Andreotti, and P. Claudin, Transition from the viscous to inertial regime in dense suspensions,

- Physical review letters **109**, 118305 (2012).
- [10] F. Boyer, É. Guazzelli, and O. Pouliquen, Unifying suspension and granular rheology, *Physical review letters* **107**, 188301 (2011).
- [11] V. Démery, Mean-field microrheology of a very soft colloidal suspension: Inertia induces shear thickening, *Physical Review E* **91**, 062301 (2015).
- [12] C. Dai, I. R. Bruss, and S. C. Glotzer, Phase separation and state oscillation of active inertial particles, *Soft matter* **16**, 2847 (2020).
- [13] R. J. Macfarlane, B. Lee, M. R. Jones, N. Harris, G. C. Schatz, and C. A. Mirkin, Nanoparticle superlattice engineering with dna, *science* **334**, 204 (2011).
- [14] W. B. Rogers, W. M. Shih, and V. N. Manoharan, Using dna to program the self-assembly of colloidal nanoparticles and microparticles, *Nature Reviews Materials* **1**, 1 (2016).
- [15] D. J. Lewis, L. Z. Zornberg, D. J. Carter, and R. J. Macfarlane, Single-crystal winterbottom constructions of nanoparticle superlattices, *Nature materials* **19**, 719 (2020).
- [16] M. Mammen, S.-K. Choi, and G. M. Whitesides, Polyvalent interactions in biological systems: implications for design and use of multivalent ligands and inhibitors, *Angewandte Chemie International Edition* **37**, 2754 (1998).
- [17] T. Sakai, S. I. Nishimura, T. Naito, and M. Saito, Influenza a virus hemagglutinin and neuraminidase act as novel motile machinery, *Scientific reports* **7**, 1 (2017).
- [18] T. Sakai, H. Takagi, Y. Muraki, and M. Saito, Unique directional motility of influenza c virus controlled by its filamentous morphology and short-range motions, *Journal of virology* **92**, e01522 (2018).
- [19] M. Müller, D. Lauster, H. H. Wildenauer, A. Herrmann, and S. Block, Mobility-based quantification of multivalent virus-receptor interactions: New insights into influenza a virus binding mode, *Nano letters* **19**, 1875 (2019).
- [20] R. Alon and S. Feigelson, From rolling to arrest on blood vessels: leukocyte tap dancing on endothelial integrin ligands and chemokines at sub-second contacts, in *Seminars in immunology*, Vol. 14 (Elsevier, 2002) pp. 93–104.
- [21] K. Ley, C. Laudanna, M. I. Cybulsky, and S. Nourshargh, Getting to the site of inflammation: the leukocyte adhesion cascade updated, *Nature Reviews Immunology* **7**, 678 (2007).
- [22] C. Korn and U. Schwarz, Dynamic states of cells adhering in shear flow: from slipping to rolling, *Physical review E* **77**, 041904 (2008).
- [23] P. C. Bressloff and J. M. Newby, Stochastic models of intracellular transport, *Reviews of Modern Physics* **85**, 135 (2013).
- [24] D. A. Hammer, Adhesive dynamics, *Journal of biomechanical engineering* **136**, 021006 (2014).
- [25] N. Dorsaz, C. De Michele, F. Piazza, and G. Foffi, Inertial effects in diffusion-limited reactions, *Journal of Physics: Condensed Matter* **22**, 104116 (2010).
- [26] F. Piazza, G. Foffi, and C. De Michele, Irreversible bimolecular reactions with inertia: from the trapping to the target setting at finite densities, *Journal of Physics: Condensed Matter* **25**, 245101 (2013).
- [27] J. P. Lee-Thorp and M. Holmes-Cerfon, Modeling the relative dynamics of dna-coated colloids, *Soft matter* **14**, 8147 (2018).
- [28] S. Marbach, J. A. Zheng, and M. Holmes-Cerfon, The nanocaterpillar’s random walk: Diffusion with ligand-receptor contacts, <https://arxiv.org/abs/2110.03112> (2021).
- [29] M. Rubinstein, R. H. Colby, *et al.*, *Polymer physics*, Vol. 23 (Oxford university press New York, 2003).
- [30] E. Miller, T. Garcia, S. Hultgren, and A. F. Oberhauser, The mechanical properties of e. coli type 1 pili measured by atomic force microscopy techniques, *Biophysical journal* **91**, 3848 (2006).
- [31] R. Y. Lim, N.-P. Huang, J. Köser, J. Deng, K. A. Lau, K. Schwarz-Herion, B. Fahrenkrog, and U. Aebi, Flexible phenylalanine-glycine nucleoporins as entropic barriers to nucleocytoplasmic transport, *Proceedings of the National Academy of Sciences* **103**, 9512 (2006).
- [32] F. B. Usabiaga, R. Delgado-Buscalioni, B. E. Griffith, and A. Donev, Inertial coupling method for particles in an incompressible fluctuating fluid, *Computer Methods in Applied Mechanics and Engineering* **269**, 139 (2014).
- [33] M. Holmes-Cerfon, Stochastic disks that roll, *Physical Review E* **94**, 052112 (2016).
- [34] Y. Bae, S. Lee, J. Kim, and H. Jeong, Inertial effects on the brownian gyrator, *Physical Review E* **103**, 032148 (2021).
- [35] B. Fogelson and J. P. Keener, Enhanced nucleocytoplasmic transport due to competition for elastic binding sites, *Biophysical journal* **115**, 108 (2018).
- [36] B. Fogelson and J. P. Keener, Transport facilitated by rapid binding to elastic tethers, *SIAM Journal on Applied Mathematics* **79**, 1405 (2019).
- [37] G. Pavliotis and A. Stuart, *Multiscale methods: averaging and homogenization* (Springer Science & Business Media, 2008).
- [38] Q. Xu, L. Feng, R. Sha, N. Seeman, and P. Chaikin, Subdiffusion of a sticky particle on a surface, *Physical review letters* **106**, 228102 (2011).
- [39] F. Cui, S. Marbach, J. Zheng, M. Holmes-Cerfon, and D. S. Pine, Comprehensive microscopic view of binding between dna-coated colloids, to appear (2021).
- [40] N. K. Sauter, M. D. Bednarski, B. A. Wurzburg, J. E. Hanson, G. M. Whitesides, J. J. Skehel, and D. C. Wiley, Hemagglutinins from two influenza virus variants bind to sialic acid derivatives with millimolar dissociation constants: a 500-mhz proton nuclear magnetic resonance study, *Biochemistry* **28**, 8388 (1989).
- [41] V. Reiter-Scherer, J. L. Cuellar-Camacho, S. Bhatia, R. Haag, A. Herrmann, D. Lauster, and J. P. Rabe, Force spectroscopy shows dynamic binding of influenza hemagglutinin and neuraminidase to sialic acid, *Biophysical journal* **116**, 1037 (2019).
- [42] R. D. Vale, T. Funatsu, D. W. Pierce, L. Romberg, Y. Harada, and T. Yanagida, Direct observation of single kinesin molecules moving along microtubules, *Nature* **380**, 451 (1996).
- [43] O. Yakovenko, V. Tchesnokova, E. V. Sokurenko, and W. E. Thomas, Inactive conformation enhances binding function in physiological conditions, *Proceedings of the National Academy of Sciences* **112**, 9884 (2015).
- [44] M. M. Sauer, R. P. Jakob, T. Lubber, F. Canonica, G. Navarra, B. Ernst, C. Unverzagt, T. Maier, and R. Glockshuber, Binding of the bacterial adhesin fimh to its natural, multivalent high-mannose type glycan targets, *Journal of the American Chemical Society* **141**, 936

- (2018).
- [45] M. M. Sauer, R. P. Jakob, J. Eras, S. Baday, D. Eriş, G. Navarra, S. Berneche, B. Ernst, T. Maier, and R. Glockshuber, Catch-bond mechanism of the bacterial adhesin fimh, *Nature communications* **7**, 1 (2016).
- [46] J. Yang, S. J. Petitjean, M. Koehler, Q. Zhang, A. C. Dumitru, W. Chen, S. Derclaye, S. P. Vincent, P. Soumillion, and D. Alsteens, Molecular interaction and inhibition of sars-cov-2 binding to the ace2 receptor, *Nature communications* **11**, 1 (2020).
- [47] A. C. Walls, Y.-J. Park, M. A. Tortorici, A. Wall, A. T. McGuire, and D. Veesler, Structure, function, and antigenicity of the sars-cov-2 spike glycoprotein, *Cell* **181**, 281 (2020).
- [48] S. Y. Park, A. K. Lytton-Jean, B. Lee, S. Weigand, G. C. Schatz, and C. A. Mirkin, Dna-programmable nanoparticle crystallization, *Nature* **451**, 553 (2008).
- [49] A. Radu, G. Blobel, and M. S. Moore, Identification of a protein complex that is required for nuclear protein import and mediates docking of import substrate to distinct nucleoporins., *Proceedings of the National Academy of Sciences* **92**, 1769 (1995).
- [50] J. X. Zhang, J. Z. Fang, W. Duan, L. R. Wu, A. W. Zhang, N. Dalchau, B. Yordanov, R. Petersen, A. Phillips, and D. Y. Zhang, Predicting dna hybridization kinetics from sequence, *Nature chemistry* **10**, 91 (2018).
- [51] I. C. Jenkins, M. T. Casey, J. T. McGinley, J. C. Crocker, and T. Sinno, Hydrodynamics selects the pathway for displacive transformations in dna-linked colloidal crystallites, *Proceedings of the National Academy of Sciences* **111**, 4803 (2014).
- [52] N. Vogel, S. Utech, G. T. England, T. Shirman, K. R. Phillips, N. Koay, I. B. Burgess, M. Kolle, D. A. Weitz, and J. Aizenberg, Color from hierarchy: Diverse optical properties of micron-sized spherical colloidal assemblies, *Proceedings of the National Academy of Sciences* **112**, 10845 (2015).
- [53] M. He, J. P. Gales, É. Ducrot, Z. Gong, G.-R. Yi, S. Sacanna, and D. J. Pine, Colloidal diamond, *Nature* **585**, 524 (2020).